Applied Surface Science 255 (2009) 8931–8934

Contents lists available at ScienceDirect

Applied Surface Science

journal homepage: www.elsevier.com/locate/apsusc

Molecular dynamics of contact behavior of self-assembled monolayers on gold using nanoindentation

Te-Hua Fang [a], Win-Jin Chang [b,*], Yu-Cheng Fan [a], Cheng-I Weng [c]

[a] Institute of Mechanical and Electromechanical Engineering National Formosa University, Yunlin 632, Taiwan
[b] Department of Mechanical Engineering Kun Shan University, Tainan 710, Taiwan
[c] Department of Mechanical Engineering National Cheng Kung University, Tainan, 710, Taiwan

ARTICLE INFO

Article history:
Received 14 June 2009
Received in revised form 23 June 2009
Accepted 23 June 2009
Available online 30 June 2009

PACS:
62.20.−x
87.15.ap

Keywords:
Self-assembled monolayer
Molecular dynamics simulation
Contact pressure

ABSTRACT

Molecular dynamics simulation is used to study nanoindentation of the self-assembled monolayers (SAMs) on an Au surface. The interaction of SAM atoms is described by a general universal force field (UFF), the tight-binding second-moment approximation (TB-SMA) is used for Au substrate, and the Lennard-Jones potential function is employed to describe interaction among the indenter, the SAMs, and the Au substrate atoms. The model consists of a planar Au substrate with n-hexadecanethiol SAM chemisorbed to the substrate. The simulation results show that the contact pressure increases as the SAMs temperature increases. In addition, the contact pressure also increases as the depth and velocity of indentation increase.

1. Introduction

In recent years, self-assembled monolayers (SAMs) on a substrate surface have attracted increasing interest for many potential technological applications such as wear protection, electronic device fabrication, biological systems, and dip-pen nanolithography [1–6]. The invention and development of scanning probe microscopy provided a powerful tool and greatly enhanced the ability to understand the patterning of SAMs. A variety of experimental methods have been used to study the physical structures and chemical properties of SAMs [7–12].

On the other hand, due to the rapid development of computer technology, molecular dynamics (MD) simulation can be very effective in simulating the performance of nanodevices, recognizing the microscopic mechanisms and offering insights into microscopic behaviors [13–20]. In addition, it is also a useful and ideal model for understanding the mechanical behaviors and structural properties of a self-organizing system [21–25]. For example, Vemparala et al. [21] utilized molecular dynamics calculations to investigate the structural properties of self-assembled alkanethiol monolayer systems concerning the effect of temperature, lattice spacing, and molecular chain length. Kapila et al. [22] investigated the friction behavior of model alkylsilane films as a function of separation between the films, temperature and the velocity of the substrate. Recently, Fang et al. [25] studied the contact behavior of SAMs deposited on gold substrate in dip-pen nanolithography and found that the contact angles decreased as the temperature increased, and the smaller the cluster size, the smaller the contact angle.

To study the mechanical properties of SAMs, nanoindentation technique is often used in the experimental tests [26,27]. In the nanoindentation test, the indenter tip generally has a radius of curvature larger than 20 nm. However, the thickness of self-assembled monolayers is generally about 2–4 nm. MD simulation may be more suitable for estimating the mechanical properties. In this paper, the nanoindentation characteristics of the SAMs on an Au surface are investigated by MD simulation. In the simulation, different capped carbon nanotubes are used for an indenter to obtain a better estimate. In addition, the effects of temperature, depth, and velocity of nanoindentation on the contact pressure of the SAMs are also studied.

2. Methodology

Fig. 1 shows that the MD model consists of a SAM on an Au substrate with a face-center-cubic (FCC) lattice and an indenter with a capped carbon nanotube. The substrate is made of single crystal Au with the (1 0 0) direction of the top surface. The atom

* Corresponding author. Tel.: +886 6 2050883; fax: +886 6 2050509.
E-mail address: changwj@mail.ksu.edu.tw (W.-J. Chang).

0169-4332/$ – see front matter © 2009 Elsevier B.V. All rights reserved.
doi:10.1016/j.apsusc.2009.06.100

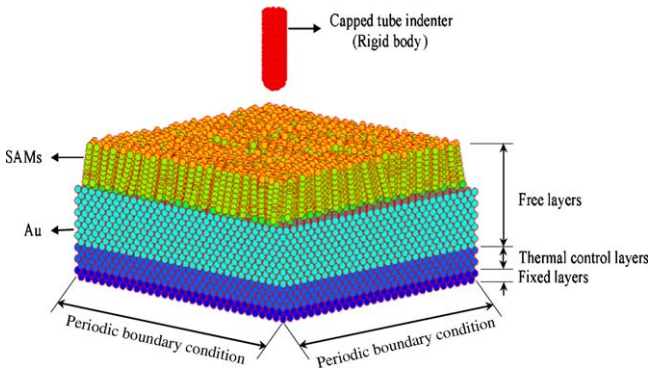

Fig. 1. Schematic of a capped tube indenter and a SAM on an Au substrate.

Table 1
The atom sum and dimension of the SAMs and Au substrate.

Materials	Au	SAMs
Size	$28 \times 30 \times 8$	$24 \times 24 \times 17$
Atom sum	26880	9792
Dimension [Å^3]	$112.2 \times 120.36 \times 30.6$	$113.45 \times 116.21 \times 47.45$

sum and dimension of the SAMs and Au substrate are listed in Table 1. The SAMs consists of the alkanethiol chain $S(CH_2)_{15}CH_3$ and is chemisorbed on an Au substrate at the temperature of 300 K. The SAMs arrays are set to 24×24. The CH_2 and CH_3 groups are treated as a single-spherical molecule to simplify as 17 united molecules per chain. Two layers of Au atoms were fixed at the substrate bottom to support the entire system and the other Au layers of thermostat atoms are set above the fixed layers to depict contact behaviors influenced by sulfur atoms during nanoindentation. A periodic boundary condition of two dimensions was imposed on plane x–y in the simulation.

The interaction of SAMs atoms is described by a general universal force field (UFF) to characterize the bonded interactions by classical potential [28]. Furthermore, the tight-binding second-moment approximation (TB-SMA), which is a many-body interatomic potential [25], that has proven capable of reproducing a variety of experimental observations [29–30] and is used in the simulation of Au substrate. The intermolecular interaction and intramolecular non-bonding interaction along the same chain are simulated by the Lennard-Jones potential [13]. The Lennard-Jones potential function is also employed to describe interaction between the SAMs and the Au substrate atoms. The capped carbon nanotubes are used for an indenter in the simulation. The indenter is assumed to be a rigid body and is built from a capped (5,5) nanotube and a capped (10,10) nanotube with a bond length of 1.41 Å. The nanotubes are composed of 240 and 530 carbon atoms for a (5,5) nanotube and a (10,10) nanotube, respectively. It is set above the Au substrate surface of 1 nm and then the indenter will approach to the substrate with a speed of 100 m/s.

3. Results and discussions

In the simulation, the snapshots of the nanoindentation process with a capped (10,10) nanotube at temperature of 300 K and indentation velocity of 100 m/s for different times are shown in Fig. 2a–c. In these figures, the indenter began to bend the SAM chain around the indentation central region before 10 ps due to the interaction among the indenter atoms and SAM chain molecules. Then, the bended SAM chains were buckled and twist under the tube indenter at 20 ps. The SAM molecules around the indentation circumference became as larger slope to the equilibrium position due to the lateral force. During the indentation process, the deformation took place along the slip (1 1 0) direction on the Au substrate as shown in Fig. 2b. This is because the contact pressure transformation and the dislocation lead to the mechanical slip behavior and stress relaxation.

The potential energy of the SAM molecules on Au substrate at the indentation depth of 1.5 nm and indentation velocity of 100 m/s for various temperature conditions are shown in Fig. 3. Before 10 ps the indentation depth of indenter tip continued to increase, the SAM molecules were affected by attractive force. The attractive force caused potential energy started to go up until it reached a critical contact region. During about 10–15 ps the indent atoms contacted and affected the SAM molecules as well as the potential energy of SAM molecules slightly decreased. After the tube full indented on the SAM molecules, the indentation load and potential energy increased until to the maximum indentation. During the hold time intervals of 25–40 ps, the slip behavior and stress relaxation took place to reduce the potential energy. The fluctuations of the potential energy were due to local structure variations of the chain molecules. After the hold time intervals of

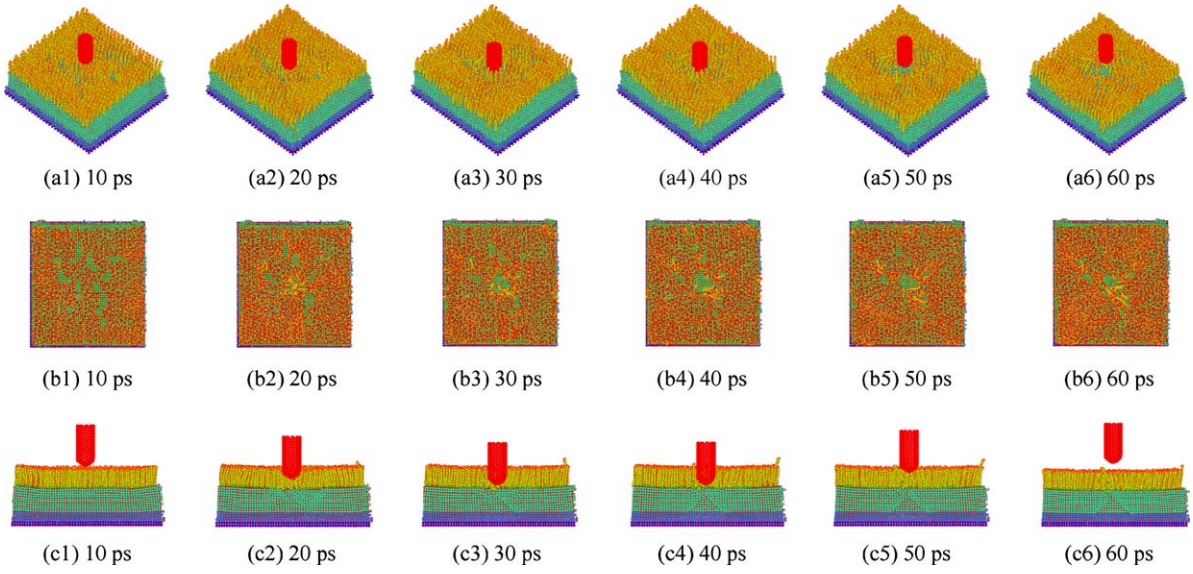

Fig. 2. The snapshots of the nanoindentation process with a capped (10,10) nanotube at temperature of 300 K and indentation velocity of 100 m/s.

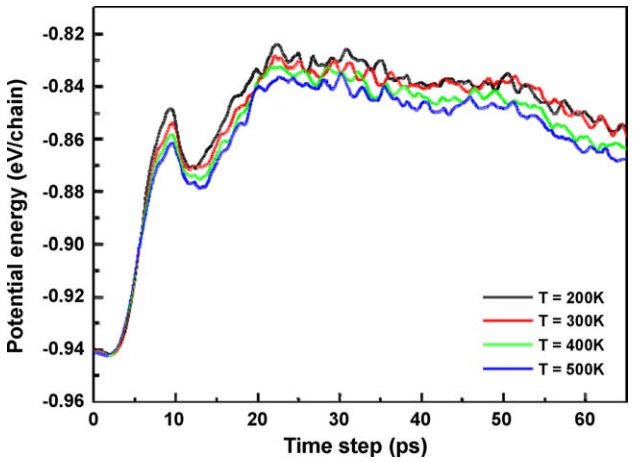

Fig. 3. The potential energy of the SAMs on Au substrate at the indentation depth of 1.5 nm and indentation velocity of 100 m/s for various temperature conditions.

40–65 ps, the tip began to unload and retain to its original position. The potential energy is seen slightly decreased due to the elastic recovery and the plastic deformation occurred. The higher temperature showed the lower potential energy. The explanation of this phenomenon from microscopic viewpoint is that higher temperature with higher kinetic energy and lower potential energy or weaker interaction as a result of high temperature [15].

The contact pressure of the SAMs on an Au surface is investigated by using the nanoindentation technique. The contact pressure is defined as the ratio of the applied load and the contact area during the indentation. Fig. 4 depicts the relationship between contact pressure and temperature of the SAMs on an Au substrate using nanoindentation technique at the indentation depth of 1.5 nm and indentation velocity of 100 m/s. As the SAMs temperature rise, the contact pressure increases due to an increase in the kinetic energy. The pressure with a (10,10) nanotube indenter is lower than that with a (5,5) one because of a larger contact area. According to the calculation, the contact radius and projected area of the (5,5) nanotube indenter are 3.37 Å and 317.2 Å^2, and those of the (10,10) nanotube indenter are 6.73 Å and 634.52 Å^2 for the indentation depth of 1.5 nm.

Fig. 5 shows the relationship between contact pressure and nanoindentation depth of the SAMs on an Au substrate using nanoindentation technique at temperature of 300 K and an indentation velocity of 100 m/s. As the depth of indentation

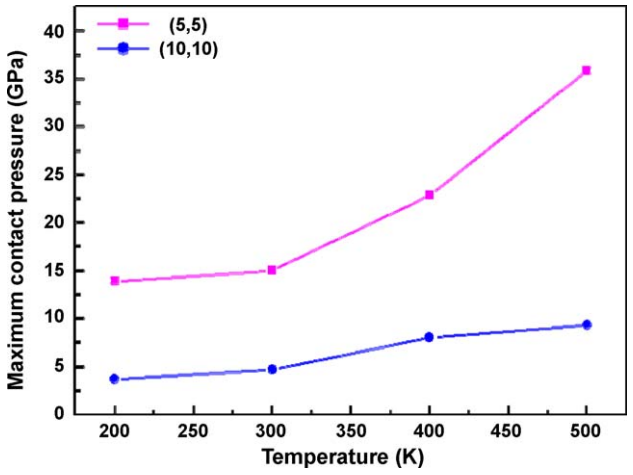

Fig. 4. The relationship between contact pressure and temperature of the SAMs on an Au substrate using nanoindentation at the indentation depth of 1.5 nm and indentation velocity of 100 m/s.

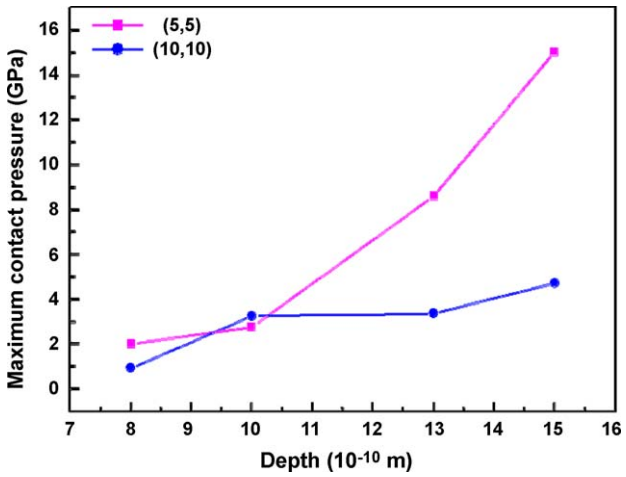

Fig. 5. The relationship between contact pressure and nanoindentation depth of the SAMs on an Au substrate using nanoindentation with different capped tube indenters at temperature of 300 K and indentation velocity of 100 m/s.

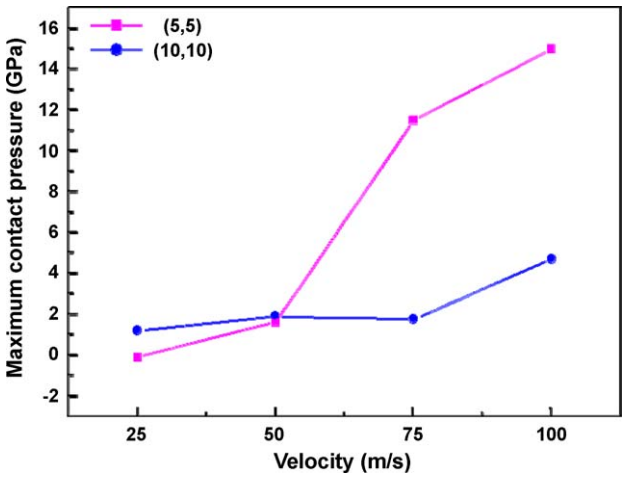

Fig. 6. The relationship between contact pressure and indentation velocity of the SAMs on an Au substrate using nanoindentation at the indentation depth of 1.5 nm and temperature of 300 K.

increases, the contact pressure increases due to an increase in the applied load. The substrate effect will occur at deeper depth. The relationship between contact pressure and indentation velocity of the SAMs on an Au substrate at the indentation depth of 1.5 nm and temperature of 300 K is shown in Fig. 6. As the indentation velocity increases, the contact pressure increases. This is because the defect in the SAMs [31] is difficult to produce when the velocity is too fast. As well, the impact energy of the indenter on the SAM surface is greater at the higher speeds.

4. Conclusions

Molecular dynamics simulation of contact pressure of the SAMs on Au using nanoindentation with different capped nanotube indenters was studied. According to the nanoindentation simulation, the results showed that the contact pressure increased as the SAMs temperature rose due to an increase in the kinetic energy. The pressure with a (10,10) nanotube indenter was lower than that with a (5,5) one. In addition, the contact pressure increased as the depth of indentation increased due to an increase in the applied load. The pressure also increased as the indentation velocity increased.

Acknowledgments

The authors wish to thank the National Science Council of Taiwan for providing financial support for this study under Projects NSC 96-2628-E-150-005-MY3 and NSC 97-2221-E-168-019-MY2.

References

[1] R.D. Piner, J. Zhu, F. Xu, S. Hong, C.A. Mirkin, Science 283 (1999) 661.
[2] T. Laiho, J.A. Leiro, J. Lukkari, Appl. Surf. Sci. 212–213 (2003) 525.
[3] S. Zhang, Nat. Biotechnol. 21 (2003) 1171.
[4] S. Monsathaporn, A novel method for photoinduced patterning of self-assembled monolayers for biological applications, Mensch & Buch Verlag, Berlin, 2004.
[5] Z. Zheng, M. Yang, Y. Liu, B. Zhang, Nanotechnology 17 (2006) 5378.
[6] M. Cichomski, J. Grobelny, G. Celichowski, Appl. Surf. Sci. 254 (2008) 4273.
[7] I. Kratochvilova, A. Zambova, J. Mbindyo, B. Razavi, J. Holakovsky, Mod. Phys. Lett. B 16 (2002) 161.
[8] W. Wang, T. Lee, M.A. Reed, Physica E 19 (2003) 117.
[9] H.B. Akkerman, B. de Boer, J. Phys.: Condens. Matter 20 (2008) 013001.
[10] R. Neil, Champness, Nat. Nanotechnol. 3 (2008) 324.
[11] F. Hubenthal, N. Borg, T. Weidner, U. Siemeling, F. Träger, Appl. Phys. A 94 (2009) 11.
[12] H. Aghaie, M.R. Gholami, M.D. Ganji, M.M. Taghavi, Curr. Appl. Phys. 9 (2009) 367.
[13] W.J. Chang, T.H. Fang, J. Phys. Chem. Solids 64 (2003) 1279.
[14] T.H. Fang, W.J. Chang, S.C. Liao, J. Phys.: Condens. Matter 15 (2003) 8263.
[15] T.H. Fang, C.I. Weng, J.G. Chang, Mater. Sci. Eng. A 357 (2003) 7.
[16] T.H. Fang, W.J. Chang, S.L. Lin, Appl. Surf. Sci. 253 (2006) 1649.
[17] Y.H. Lin, T.C. Chen, Appl. Phys. A 92 (2008) 571.
[18] W.J. Lee, S.P. Ju, C.H. Cheng, Langmuir 24 (2008) 13440.
[19] M.T. Knippenberg, P.T. Mikulski, B.I. Dunlap, J.A. Harrison, Phys. Rev. B 78 (2008) 235409.
[20] T.H. Fang, C.D. Wu, W.J. Chang, S.S. Chi, Appl. Surf. Sci. 255 (2009) 6043.
[21] S. Vemparala, B.B. Karki, R.K. Kalia, A. Nakano, P. Vashishta, J. Chem. Phys. 121 (2004) 4323.
[22] V. Kapila, P.A. Deymier, S. Raghavan, Modelling Simul, Mater. Sci. Eng. 14 (2006) 283.
[23] C.D. Wu, J.F. Lin, T.H. Fang, Comp. Mater. Sci. 39 (2007) 808.
[24] P. Tian, Annu. Rep. Prog. Chem., Sect. C 104 (2008) 142.
[25] T.H. Fang, W.J. Chang, C.D. Wu, Microelectron. Eng. 85 (2008) 223.
[26] C.W. Chang, J.D. Liao, Nanotechnology 19 (2008) 315703.
[27] D.J. Kang, D.H. Han, D.P. Kang, J.W. Yoo, B.U. Kim, Opt. Express 16 (2008) 18320.
[28] A.K. Rappe, C.J. Casewit, K.S. Colwell, W.A. Goddard, W.M. Skiff, J. Am. Chem. Soc. 114 (1992) 10024.
[29] L. Ǵomez, H.T. Diep, Phys. Rev. Lett. 74 (1995) 1807.
[30] J.J. de Miguel, R. Miranda, J. Phys.: Condens. Matter 14 (2002) R1063.
[31] C. Vericat, M.E. Vela, R.C. Salvarezza, Phys. Chem. Chem. Phys. 7 (2005) 3258.